Visible light absorption of (Fe, C/N) co-doped $NaTaO_3$: DFT+U*

Peng-Li Tian(田鹏莉)[1], Zhen-Yi Jiang(姜振益)[1,†], Xiao-Dong Zhang(张小东)[1,2,‡], Bo Zhou(周波)[1], Ya-Ru Dong(董亚茹)[1], and Rui Liu(刘睿)[3]

[1] *Institute of Modern Physics, Northwest University, Xi'an* 710069, *China*
[2] *Science and Technology on Thermostructure Composite Materials Laboratory, Northwestern Polytechnical University, Xi'an* 710072, *China*
[3] *Shaanxi Lingyun Electrics Group Co., Ltd., Baoji* 721006, *China*

(Received 27 February 2017; revised manuscript received 20 April 2017; published online 20 June 2017)

The effects of Fe–C/N co-doping on the electronic and optical properties of $NaTaO_3$ are studied with density functional theory. Our calculations indicate that mono-doped and co-doped sodium tantalate are both thermodynamically stable. The co-doping sodium tantalate can reduce the energy band gap to a greater degree due to the synergistic effects of Fe and C (N) atoms than mono-doping sodium tantalate, and has a larger optical absorption of the whole visible spectrum. The band alignments for the doped $NaTaO_3$ are well positioned for the feasibility of hydrogen production by water splitting. The Fe–C co-doping can enhance the absorption of the visible light and its photocatalytic activity more than Fe–N co-doping due to the different locations of impurity energy levels originating from their p–d hybridization effect.

Keywords: codoping, DFT+U method, electronic structure, optical properties

PACS: 71.15.Mb, 71.27.+a, 74.25.Jb **DOI:** 10.1088/1674-1056/26/8/087102

1. Introduction

Hydrogen, as a clean and renewable fuel, is one of the candidates to replace the traditional fossil fuels. Photocatalytic water splitting for H_2 has been considered as a promising approach to the environmentally friendly production of hydrogen; however, a suitable photocatalyst is essential. Among various photocatalysts, $NaTaO_3$ (perovskite-type alkali tantalate) has been extensively studied as a prospective photocatalyst for the water splitting reaction under UV radiation[1–3] due to its excellent properties, such as controllable structure, prominent photocatalytic activity and fine thermal stability.[4,5] The wide band edges of $NaTaO_3$ straddle the water redox potential levels, which is necessary for hydrogen production by photocatalytic water splitting. The delocalized nature of photoexcited electrons can promote the hydrogen generation in $NaTaO_3$.[6–8] However, the absorption of $NaTaO_3$ is limited in the UV range, which only accounts for 5% of the solar spectrum,[9] due to its large band gap ($E_g = 4.1$ eV[6]). In addition, the photoexcited electron-hole pairs in $NaTaO_3$ are relatively easy to recombine,[10–12] which impedes the enhancement of hydrogen production. Therefore, two critical factors for promoting the hydrogen generation are how to narrow the energy band gap and how to reduce the recombination of electron-hole pairs.

Recently various attempts such as ion doping, semiconductor coupling and dye sensitizing[13–16] have been developed to enhance the photocatalytic effect of semiconductor photocatalysts. Among them, doping ions[17,18] is a promising approach to improving visible light absorption. For instance, Liu *et al.*[19] proposed that N-doped $NaTaO_3$ exhibits higher photocatalytic activities than the pure $NaTaO_3$. The reason is that the newly formed intra-bandgap states are close enough to the conductor band (CB) edge, which may prevent charges from being recombined. Meanwhile, Wang *et al.*[20] demonstrated that the C (N) p orbital mixing with O p orbital increases the width of the valance band (VB), resulting in significantly narrowing the band gap when doped with C (N). In addition, Zhou *et al.*[21] reported that the band gap of Fe doped $NaTaO_3$ is narrowed to 2.03 eV indicated from the DFT calculations and leads to an obvious red-shift of light absorption. However, the improvement of photocatalytic efficiency by mono-doping is still limited. A natural ideal is to combine the advantages of a metal ion and those of a nonmetal ion to further improve its ability to produce hydrogen by the co-doping method.

Although there are some intensive studies about the photocatalytic effect of doped $NaTaO_3$, the electronic natures of these doped systems are not well understood. Moreover, to the best of our knowledge, there are few corresponding theoretical researches that uncover the mechanism of cation-anion co-doping, which has been proved to be effective in other oxide systems, such as TiO_2.[22] Hence we use the density functional theory (DFT) plus the U method to investigate the mono- and

*Project supported by the National Natural Science Foundation of China (Grant Nos. 51572219 and 11204239), the Project of the Natural Science Foundation of Shaanxi Province, China (Grant Nos. 2015JM1018, 2013JQ1018, and 15JK1714), the Project of Natural Science Foundation of Department of Education of Shaanxi Province, China (Grant No. 15JK1759), and the Science Foundation of Northwest University of China (Grant No. 12NW06).

†Corresponding author. E-mail: jiangzy@nwu.edu.cn
‡Corresponding author. E-mail: zhangxiaodong@nwu.edu.cn

© 2017 Chinese Physical Society and IOP Publishing Ltd

co-doping effects of C, N, and Fe in $NaTaO_3$, which can improve our understanding of the mechanism of cation-anion co-doping.

2. Computational details

Our calculations were performed using the projector augmented wave (PAW) pseudopotentials[23,24] with a plane-wave basis set as implemented in the Vienna *Ab initio* Simulation Package (VASP)[25] code. The exchange correlation potential was treated by the generalized gradient approximation (GGA) with the Perdew–Becke–Erenfest parameterization (known as GGA-PBE).[26] The electron wave function was expanded in plane waves up to a cutoff energy of 500 eV. The Brillouin zone (BZ) integrations were carried out by using the special *k*-point sampling of the Monkhorst–Pack[27] type. The dense *k*-point grids 7×7×6 were used for $NaTaO_3$. The chosen plane-wave cutoff and the number of *k* points were carefully checked to ensure the total energy converged to better than 1 meV per formula unit (f.u.). Both the atomic positions and the cell parameters were optimized simultaneously until residual forces were reduced to below 0.01 eV/Å. The supercell approach has been employed to study the pure and doped systems on the electronic structure of $NaTaO_3$. A 2×2×2 supercell with 160 atoms has been constructed.

We used C (N) to replace O and substituted Fe for the Ta site in the lattice. The ionic radius of Fe (0.72 Å) is close to that of Ta^{5+} (0.64 Å) while it is largely different from that of Na^+ (1.39 Å), so we preferred to use Fe to replace the Ta^{5+} rather than Na^+ in the present study.[21]

It is generally known that the standard DFT method usually underestimates the band gap for a semiconductor, while the DFT+U approach can introduce an on-site correction to describe the localized d electrons. Therefore, we adopted the DFT+U method for Ta 5d electrons to calculate the electronic and optical properties in order to obtain an accurate theoretical band gap. As is well known, the spherically average Hubbard parameter U describes the extra energy while the parameter J denotes the screened exchange energy. The effective Hubbard parameter $U_{\text{eff}} = U - J$ is required to include the on-site Coulomb repulsion for each affected orbital.[28] The $U = 8.00$ eV and $J = 0.95$ eV were found to well reproduce the experimental band gap.

3. Results and discussion

3.1. Structural optimization and formation energy

$NaTaO_3$ has an orthorhombic structure with space group *Pbnm*. The structure of the pure $NaTaO_3$ is optimized using the experimental data as initial values. The calculated lattice parameters are $a = 5.50$ Å, $b = 5.57$ Å, and $c = 7.83$ Å, which are in good agreement with experimental values.[29] These results indicate that our calculation methods are reasonable. All the doped systems are constructed from the relaxed (2×2×2) 160-atom orthorhombic $NaTaO_3$ supercell as shown in Fig. 1. The Ta cation is 6-fold coordinated with six O anions, forming a tilted octahedron, with the Na cation located in the center of it. The mono-doped systems are modeled by replacing one of the O or Ta atoms by C/N or Fe atoms, respectively (see Fig. 1). At the same time, one O atom and one Ta atom are substituted by one C/N and one Fe atom for co-doping (see Fig. 1). After optimization, the distance between Ta and O atoms is 1.996 Å in pure $NaTaO_3$. However, for Fe–C/N co-doped $NaTaO_3$, the calculated Fe–C and Fe–N bond lengths are 1.595 Å and 1.566 Å, respectively, indicating a slight contraction in comparison with the Ta-O bond length. The distance between Fe and N atoms is unchanged before and after the optimization, however, the Fe–C bond decreases by 0.402 Å after optimization. This suggests that the Fe and C atoms are easier to close each other than Fe and N atoms. So many differences may result in a substantial difference in the electronic properties. To investigate the relative stabilities of the doped systems, the formation energies E_{f} are calculated by the following equations:

$$E_{\text{f}} = E_{\text{monodoped}} - E_{\text{pure}} - \mu_X + \mu_Y, \tag{1}$$

$$E_{\text{f}} = E_{\text{codoped}} - E_{\text{pure}} - \mu_M + \mu_{\text{O}} - \mu_{\text{Fe}} + \mu_{\text{Ta}}, \tag{2}$$

$$\mu_{\text{Na}} + \mu_{\text{Ta}} + 3\mu_{\text{O}} = \mu_{\text{NaTaO}_3}, \tag{3}$$

$$3\mu_{\text{Fe}} + 4\mu_{\text{O}} = \mu_{\text{Fe}_3\text{O}_4}, \tag{4}$$

$$\mu_{\text{C}} + 2\mu_{\text{O}} = \mu_{\text{CO}_2}, \tag{5}$$

where X = C, N, Fe; Y = O, Ta; M = C, N; $E_{\text{monodoped}}$, E_{codoped}, and E_{pure} are the total energies of the mono-doped, co-doped, and pure $NaTaO_3$, respectively; $\mu_{X/Y/M/\text{O/Fe/Ta}}$ represent the chemical potentials for C, N, Fe, O, and Ta atoms, respectively. The chemical potential of the constituent elements must satisfy the relationship from Eq. (3) for $NaTaO_3$. It should be mentioned that the formation energy is not fixed but dependent on the growth condition. The O-rich and the

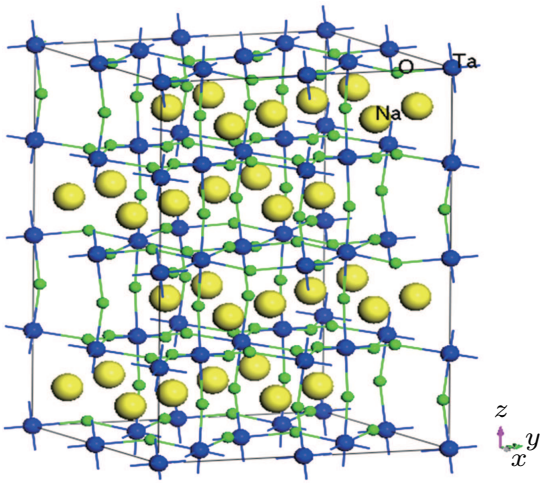


Fig. 1. (color online) Supercell structure for orthorhombic $NaTaO_3$. The blue, green, and yellow spheres represent Ta, O, and Na atoms, respectively. The lattice sites of the dopant are marked by Ta and O.

Ta-rich conditions are considered to be calculated. Under the environment of an O-rich condition, μ_O is calculated from the energy of an oxygen molecule ($\mu_O = \frac{1}{2}\mu_{O2}$) and μ_{Ta} is obtained from Eq. (3). At the same time, μ_{Ta} is determined from the energy of the Ta atom in the bulk crystal and μ_O is obtained from Eq. (3) for the case of a Ta-rich condition. The μ_{Na} is determined from the energy of the Na atom in the bulk crystal. The μ_N has been calculated as the energy of the nitrogen atom in the diatomic molecules in the gas phase and the chemical potentials of other atoms are calculated from Eqs. (4) and (5). The calculated defect formation energies for all mono-doped and co-doped $NaTaO_3$ under the O-rich and Ta-rich conditions are listed in Table 1. The lower the formation energy, the more stable the doping structure is. As shown in Table 1, the negative formation energy indicates that all these doped systems are thermodynamically stable. For the Fe–C co-doped system, the formation energy is −5.55 eV under the Ta-rich condition, which is more suitable than the O-rich condition. However, for the Fe–N co-doped system, the formation energy is −5.64 eV, which is suitable under the O-rich condition. In a word, all of the doped structures are reasonably stable and worth studying.

Table 1. Defect formation energies of different doping structures (in unit eV).

	Pure $NaTaO_3$	C@O	N@O	Fe@Ta	C@O&Fe @Ta	N@O&Fe@Ta
E_f (O-rich)	–	–6.71	-0.53	–9.05	–0.09	–5.64
E_f (Ta-rich)	–	–19.03	–4.63	–2.20	–5.55	–3.76

3.2. Electronic structures

3.2.1. Pure $NaTaO_3$

The calculated energy band structures of pure $NaTaO_3$ by the DFT method and the DFT+U method are shown in Fig. 2, respectively.

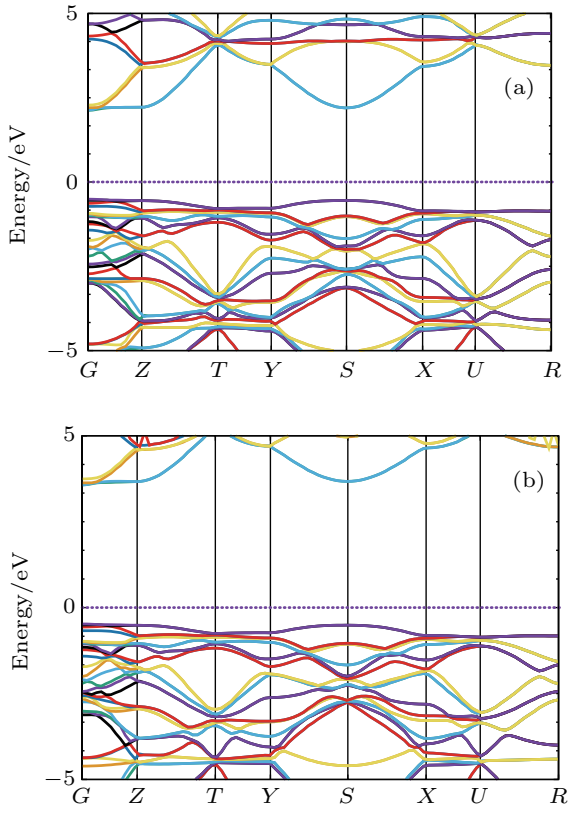


Fig. 2. (color online) Band structures of pure $NaTaO_3$ calculated by (a) DFT method and (b) DFT+U method.

The calculated direct band gap (Γ–Γ) is 2.7 eV (see Fig. 2(a)), which is close to the value of 2.89 eV calculated by Wang *et al.*,[30] but is much smaller than the experimental value (3.98 eV[19]) due to the well-known shortcoming of the standard DFT approach. As mentioned, the DFT calculations cannot accurately describe the Ta-d electrons, so we employ the DFT+U method to calculate the band structure of $NaTaO_3$. The DFT+U calculation gives the band gap of 3.92 eV (see Fig. 2(b)), which is in good agreement with the experimental observation (3.98 eV[19]). It should be emphasized that the DFT+U approach results in the improvement of the electronic structures compared with the traditional DFT method. Therefore, the DFT+U method is employed for the following calculations.

In order to clarify the orbital information of $NaTaO_3$, the total density of states (DOS) and partial density of states (PDOS) of pure $NaTaO_3$ are calculated and plotted in Fig. 3. The PDOS shows that the valence band maximum (VBM) is principally O 2p orbital in character and the conduction band minimum (CBM) is mainly composed of Ta 5d orbital. It elucidates that the electrons transferring from O 2p to Ta 5d states is the main reason for optical absorption, which is consistent with previous work.[20]

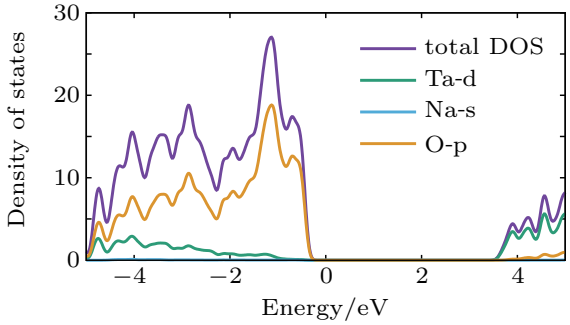


Fig. 3. (color online) Total density of states (TDOS) and partial density of states (PDOS) of pure $NaTaO_3$ based on DFT+U calculations.

3.2.2. Mono-doping effects of C, N, and Fe on $NaTaO_3$

Generally, in order to shift the conduction band downward for narrowing the band gap, the metal dopant d orbital

energy should be lower than that of the Ta 5d. On the other hand, we need the non-metal dopants to have a higher 2p orbital energy than that of O 2p to shift the valence band upward.

We calculate a series of energy band structures of C-doped (see Fig. 4(a)), N-doped (see Fig. 4(c)), and Fe-doped (see Fig. 4(e)) $NaTaO_3$ systems. For the C-doped model, we find that the impurity energy states appear in the forbidden gap. The same phenomenon is also observed in the N-doped system. As a matter of fact, the introduction of the C or N dopant due to their higher energy levels of p orbital than that of O reduce the band gap by 0.66 eV or 1.14 eV, respectively, compared with undoped $NaTaO_3$. The N 2p states form the VBM while C 2p states are just above the VBM to act as impurity levels. Thus, the narrowing of the band gap is helpful for allowing $NaTaO_3$ to absorb near-visible-range light. For Fe-doped $NaTaO_3$ (see Fig. 4(e)), both shallow levels and deep levels are present within the band gap, making the band gap much smaller than that of the pure $NaTaO_3$. The phenomenon shows a similar trend to that indicated in the previous study of Zhou *et al*.[21] The deep levels are disadvantageous factors for the light absorption efficiency, so co-doping with anion should be a choice for overcoming the negative factor of deep impurity energy levels.

Besides, the total density of states (DOS) and projected density of states (PDOS) of the doped systems are calculated to elucidate the orbital information in detail. For the N-doped model (see Fig. 4(d)), the N 2p orbitals are split into a higher degenerated *e* orbital and a lower non-degenerated *a* orbital. The *e* orbital is just above VBM of pure $NaTaO_3$, nevertheless the *a* orbital is located within the valence bands. In particular, the N 2p orbitals can mix well with the O 2p orbitals at the VBM for the reduction of the band gap while CBM is not affected by this doping, which is similar to the other theoretical results.[9,20] These impurity states make possible the electrons transferring from VB to the CB even with light of lower energy than in the case of pure $NaTaO_3$, which extends the absorption edge to the visible light range (see Fig. 6).

For the C-doped model (see Fig. 4(b)), the C 2p orbitals are split into three states, which shows a similar trend to that indicated by the previous study of Wang *et al*.[20] Its higher state stays at about 0.14 eV above the Fermi level, while another two states are located at about 0.08 eV and −1.29 eV below the Fermi level, respectively. The C 2p states bestow the VBM with a higher oxidation ability to reduce the band gap and form a shallow acceptor level above the top of the VB to help CB accept the photoexcited electrons from the VB with lower energy, and then enhance the utilization of visible light effectively. The narrower band gap would make the absorption edge of C-$NaTaO_3$ move to the visible light range (see Fig. 6) in comparison with that of pure $NaTaO_3$, which is well consistent with the experiment measurements.[31]

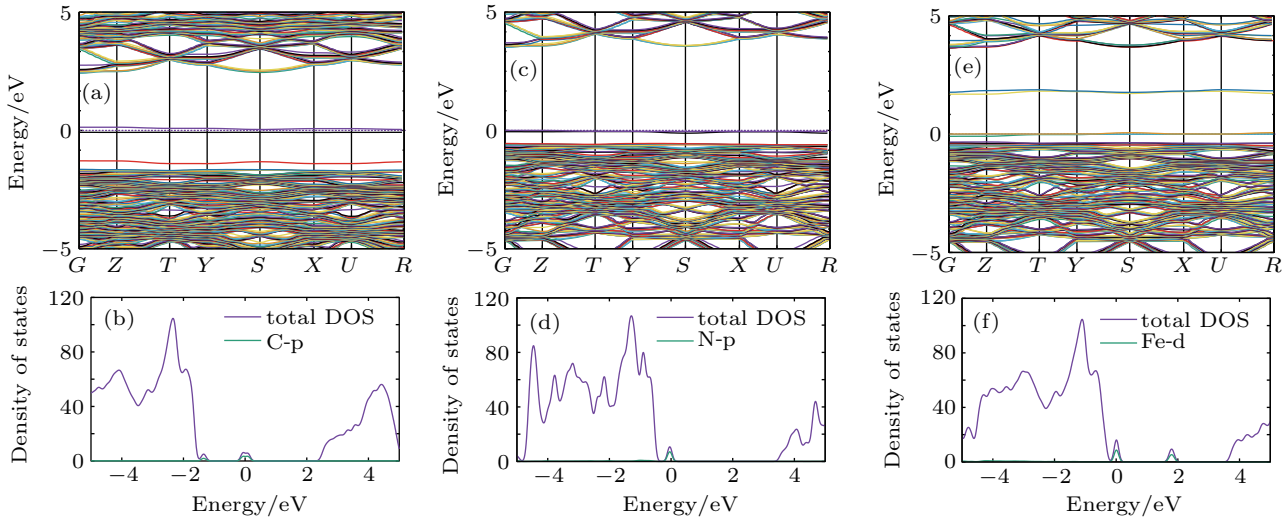


Fig. 4. (color online) Band structures of (a) C-doped $NaTaO_3$, (c) N-doped $NaTaO_3$, and (e) Fe-doped $NaTaO_3$; total densities of states (TDOSs) and partial densities of states (PDOSs) of (b) C-doped $NaTaO_3$, (d) N-doped $NaTaO_3$, and (f) Fe-doped $NaTaO_3$.

For Fe-doped $NaTaO_3$ (see Fig. 4(f)), two nearly degenerated states (1.69 eV and 1.77 eV above the Fermi level), another two nearly degenerated states (0.009 eV and 0.007 eV below the Fermi level) and one state (0.090 eV below the Fermi level) contribute to not only the VBM but also the CBM, which are responsible for the gap narrowing and the enhanced absorption of visible light (see Fig. 6). The unoccupied state above the VB from hybridization of Fe 3d and O 2p states can act as a middle springboard, which allows the electrons with lower energy to transfer gradually from the valence band to the conduction band. On the other hand, the impurity energy levels can transfer its local electrons to the CBM energy levels by absorbing the photo electrons, resulting in the absorption of longer-wavelength (previous 650 nm[21]) visible-light. However, the deep energy levels in the middle of the band gap may act as a recombination center on the basis of the report by Gai

et al.,[22] which hinders the separation and migration of the photoexcited electron-hole pairs, thus limiting the solar energy conversion for the production of hydrogen to some extent. The same phenomenon has also been observed in the other theoretical results.[21,32] Our present calculations provide an accurate trend for the following calculations. In a word, our theoretical results indicate that mono-doped $NaTaO_3$ is still an efficient catalyst for splitting water under visible light to some extent. However, the improvement of the photocatalytic efficiency for the mono-doping $NaTaO_3$ is quite limited, in spite of significant enhancement of the visible light absorption (see Fig. 6).

3.2.3. Co-doping effects of Fe–C, Fe–N on $NaTaO_3$

The co-doping technique has been proved to be efficient in producing visible light photocatalyst and reducing its recombination rate.[33] Here, we mainly study the co-doping effects of Fe–C and Fe–N co-doped $NaTaO_3$ to explain the above theory. The calculated band energy structures for the Fe–C and Fe–N co-doped $NaTaO_3$ are shown in Figs. 5(a) and 5(c). It is clearly observed that numerous hybrid impurity states emerge in the forbidden gap compared with the mono-doped $NaTaO_3$. Their band gaps have been reduced obviously to 2.78 eV and 2.65 eV, respectively, which may lead to an obvious red-shift of light absorption and then the influence of the impurity state on the photocatalytic activity. Hence the Fe–C and Fe–N co-doped $NaTaO_3$ will be better photocatalysts for hydrogen production than the mono-doped $NaTaO_3$.

We also calculate the density of states (DOS) and projected DOS (PDOS) of the co-doped system to further illustrate our point of view. The calculated DOS and PDOS are displayed in Figs. 5(b) and 5(d). For Fe–C co-doped $NaTaO_3$, the band gap is greatly reduced compared with pure $NaTaO_3$. The VBM has a small rise while the CBM has an obvious decrease of about 0.59 eV, which is mainly due to the hybridization effects of Fe 3d and C 2p states in CBM. As expected, the unoccupied impurity states above the VB, with the synergistic effect of Fe 3d states and C 2p states, are related to the enhancement of visible light absorption (see Fig. 6). On one hand, part of the electrons in the VBM transfer to the CBM through the impurity states step by step. They jump to the conduction band with the narrowed band gap directly, resulting in a decrease of the photoexcited energy. Our calculated results also indicate that Fe–C co-doping can red-shift the light absorption edge into the visible light range (see Fig. 6) due to the narrowed band gap. It is worth noting that the Fe 3d states and C 2p states can hybridize easily to produce the hybrid orbitals, causing the deep energy levels to shift up to the CBM and then form the shallow levels, which can suppress the recombination of the electron-hole pairs. However, some deep levels still stay in the band gap, so the electron-hole recombination is not totally suppressed although Fe–C co-doping is better than Fe–N co-doping as shown in the following paragraph.

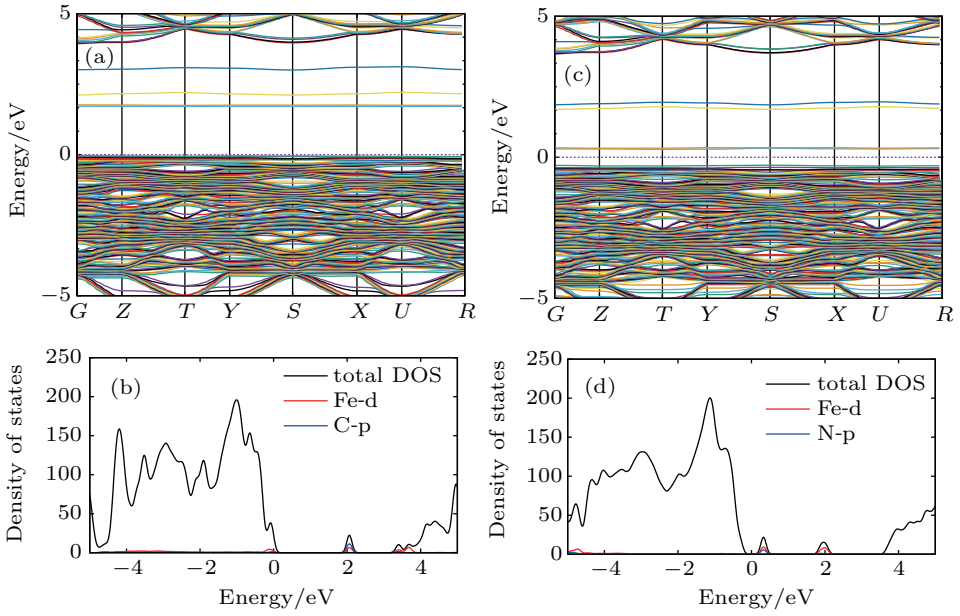


Fig. 5. (color online) Band structures of (a) Fe–C co-doped $NaTaO_3$ and (c) Fe–N co-doped $NaTaO_3$; total densities of states (TDOSs) and partial densities of states (PDOSs) of (b) Fe–C co-doped $NaTaO_3$ and (d) Fe–N co-doped $NaTaO_3$.

For Fe–N co-doped $NaTaO_3$, the PDOS plot indicates that the hybrid N 2p, Fe 3d, and O 2p states, acting as impurity levels, contribute to the top of the valence band and are responsible for obvious gap narrowing, resulting in the improvement of absorption in the whole visible light region (see Fig. 6). One possible reason is that the Fe-3d orbital hybridizes with the N-2p orbital, forming a shallow p–d hybridized orbital and leading to the narrowed band gap and thus the improvement of absorption of visible light. The calculated results are consistent with the experimental measurements.[34] How-

ever, the deep level formed by Fe-3d orbitals in the forbidden gap is detrimental to the light absorption efficiency. Clearly, the co-doped system holds higher photocatalytic activity than the mono-doped system. Fe–C co-doping is better than Fe–N co-doping due to different locations of impurity energy levels originating from their p–d hybridization effect.

3.3. Optical properties

To investigate the influences of mono-doping and co-doping on the optical property, we calculate the optical absorption spectra for C, N, Fe, and Fe–C, Fe–N-doped $NaTaO_3$ and compare them with those for the pure $NaTaO_3$ as plotted in Fig. 6.

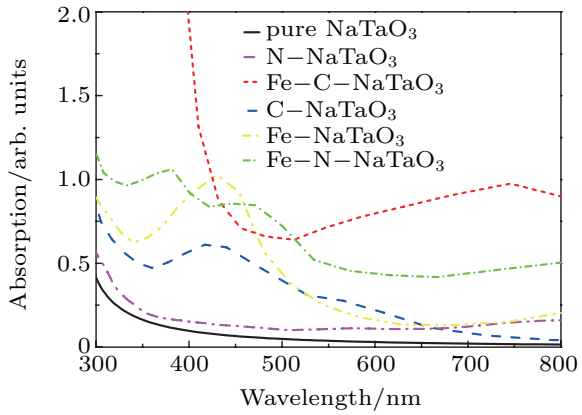


Fig. 6. (color online) Optical absorption spectra of pure and doped $NaTaO_3$.

It is clear that the pure $NaTaO_3$ shows no response to the visible light and only responds to UV light ($\lambda < 390$ nm) due to its wide band gap. Compared with the pure system, the C (Fe) doped system displays a good optical absorption, particularly in the visible light region due to the narrowing of the band gap and the synergistic effect of impurity energy levels, which is well consistent with the experimental optical absorption spectrum.[21,31] On the contrary, the N doping fails to exhibit an excellent visible light absorption, however, the absorption shift towards the visible region is quite significant, and then the results are consistent with the results of a previous theoretical study of Modak *et al.*[9] With the help of the Fe dopant, the light absorption activities of Fe–C, Fe–N-doped $NaTaO_3$ rise dramatically, which demonstrates that co-doping is superior to mono-doping to some extent. It is shown that an obvious red-shift appears in Fe–C-doped $NaTaO_3$, which facilitates the utilization of sunlight in the whole visible light region compared with the case of pure (mono-doped) $NaTaO_3$. It is shown that the energy band structures of Fe–C, Fe–N-doped $NaTaO_3$ are of benefit to the improvement of optical absorption since they possess the minimum band gap compared with others, which are shown in Figs. 5(a) and 5(c). Moreover, the synergistic effects of the C (N) 2p, Fe 3d, O 2p, and Ta 5d lead to a reduction of the photoexcited energy, which, in view of the electronic structure, may be responsible for the red-shift phenomenon of the optical absorption edge in co-doped $NaTaO_3$. Hence, the co-doping will work better in gap narrowing and the absorption of longer-wavelength visible light. The calculated result of the Fe–N co-doped system is consistent with the experimental result of Zhao *et al.*[34]

3.4. Photocatalytic activity

Water can be decomposed into H_2 and O_2 when both oxidation and reduction of energy levels of water are within the band gap of pure $NaTaO_3$. The locations of the band edges should be appropriate for a spontaneous redox process while modifying the band gap. The CBM position is 1.1 eV higher than the hydrogen reduction level while the VBM is 1.77 eV lower than the water oxidation level[6] for pure $NaTaO_3$. The CBM and VBM values for both the mono-doped and co-doped systems are calculated by designating the core-level as a reference point, which is nearly fixed. Our calculations show that the locations of the band edges are favorable for the water reduction and oxidation processes for doped systems in Fig. 7.

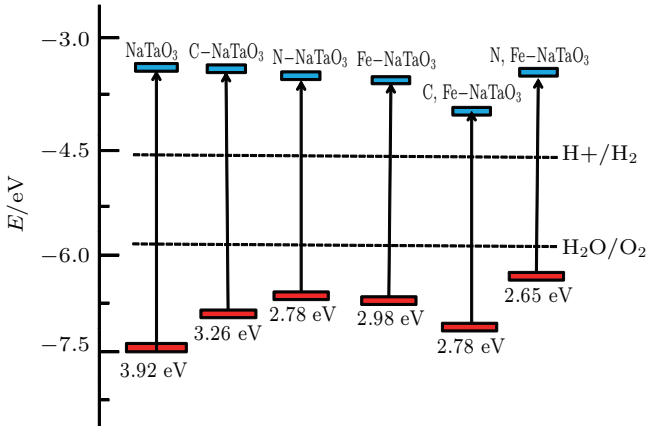


Fig. 7. (color online) Calculated VBM and CBM positions of mono-doped and co-doped $NaTaO_3$ with reference to the respective experimental values of undoped $NaTaO_3$.

For the C-doped system, the VBM is 1.24 eV lower than the O_2/H_2O level and the CBM is 1.13 eV higher than the H^+/H_2 level. It is also possible for the N-doped $NaTaO_3$ photocatalyst to produce H_2 and O_2 with its valence band edge moved upward by 0.36 eV above that of the C-doped system. However, for the Fe-doped system, there is a small downward shift of the CBM while the VBM is moved upward by 0.68 eV with respect to that of pure $NaTaO_3$. The calculated potentials of VBM and CBM of Fe–C co-doped $NaTaO_3$ are more positive and negative than the reduction level and oxidation level of water by 1.15 eV and 0.57 eV, respectively. Thus, the co-doping Fe and C into $NaTaO_3$ is expected to be efficient for photocatalytic splitting of water under visible light. Although it is feasible for Fe–N-co-doped $NaTaO_3$ to generate H_2 and O_2, the localized states in the band gap may work as a

recombination center, which is undesirable for photocatalytic purposes.

4. Conclusions

Density functional theory is used to study the effects of Fe–C co-doping and Fe–N co-doping on $NaTaO_3$. Our results show that all co-doped structures are quite stable due to their negative formation energies that are calculated. The energy band gaps of the co-doped systems are significantly reduced since Fe 3d orbital energy can lower the CBM and at the same time C 2p (N 2p) orbital energy can lift the VBM. The reduced band gap of co-doped $NaTaO_3$ leads to the appearance of an obvious red-shift, which enhances the utilization rate of visible light for hydrogen production by water splitting. In addition, the C 2p orbitals interact with the Fe 3d orbitals, forming the hybridized orbitals, which may depress the recombination of photoexcited electron-hole pairs. The positions of the band edges of doped $NaTaO_3$ are appropriate for overall water splitting. Our calculated results also indicate that the Fe–C co-doping is better than Fe–N co-doping for absorption improvement of the visible light and enhances the photocatalytic activity. Therefore, the significant enhancement of the visible light absorption and depression of the electron-hole recombination rate are two key factors for improving the photocatalytic activity of Fe–C co-doped $NaTaO_3$.

References

[1] Bouafia H, Hiadsi S, Abidri B, Akriche A, Ghalouci L and Sahli B 2013 *Comput. Mater. Sci.* **75** 1
[2] Liu J W, Chen G, Li Z H and Zhang Z G 2007 *Int. J. Hydrogen Energy* **32** 2269
[3] Kato H, Asakura K and Kudo A 2003 *J. Am. Chem. Soc.* **125** 3082
[4] Kanhere P, Zheng J W and Chen Z 2012 *Int. J. Hydrogen Energy* **37** 4889
[5] Su Y G, Peng L M, Guo J W, Huang S S, Lv L and Wang X J 2014 *J. Phys. Chem. C* **118** 10728
[6] Kato H and Kudo A 2001 *J. Phys. Chem. B* **105** 4285
[7] Kanhere P D, Zheng J W and Chen Z 2011 *J. Phys. Chem. C* **115** 11846
[8] Yamakata A, Ishibashi T A, Kato H, Kudo A and Onishi H 2003 *J. Phys. Chem. B* **107** 14383
[9] Modak B, Srinivasu K and Ghosh S K 2014 *J. Phys. Chem. C* **118** 10711
[10] Meyer T, Priebe J B, da Silva R O, Peppel T, Junge H, Beller M, Brückner A and Wohlrab S 2014 *Chem. Mater.* **26** 4705
[11] Li X and Zang J L 2009 *J. Phys. Chem. C* **113** 19411
[12] An L J, Park Y H, Sohn Y G and Onishi H S 2015 *J. Phys. Chem. C* **119** 28440
[13] Reddy K H, Martha S and Parida K M 2012 *RSC Adv.* **2** 9423
[14] An L J and Onishi H 2015 *ACS Catal.* **5** 3196
[15] Iwase A, Kato H and Kudo A 2013 *Appl. Catal. B: Environ.* **136** 89
[16] Hu C C and Teng H 2007 *Appl. Catal. A: Gen.* **331** 44
[17] Kudo A and Kato H 2000 *Chem. Phys. Lett.* **331** 373
[18] Xu D B, Chen M, Song S Y, Jiang D L, Fan W Q and Shi W D 2014 *CrystEngComm* **16** 1384
[19] Liu D R, Wei C D, Xue B, Zhang X G and Jiang Y S 2010 *J. Hazard. Mater.* **182** 50
[20] Wang B C, Kanhere P D, Chen Z, Nisar J, Pathak B and Ahuja R 2013 *J. Phys. Chem. C* **117** 22518
[21] Zhou X, Shi J Y and Li C 2011 *J. Phys. Chem. C* **115** 8305
[22] Gai Y Q, Li J B, Li S S, Xia J B and Wei S H 2009 *Phys. Rev. Lett.* **102** 036402
[23] Blöchl P E 1994 *Phys. Rev. B* **50** 17953
[24] Kresse G and Joubert D 1999 *Phys. Rev. B* **59** 1758
[25] Kresse G and Hafner J 1993 *Phys. Rev. B* **47** 558
[26] Perdew J P, Chevary J A, Vosko S H, Jackson K A, Pederson M R, Singh D J and Fiolhais C 1992 *Phys. Rev. B* **46** 6671
[27] Monkhorst H J and Pack J D 1976 *Phys. Rev. B* **13** 5188
[28] Arroyo-de Dompablo M E, Morales-García A and Taravillo M 2011 *J. Chem. Phys.* **135** 054503
[29] Shanker V, Samal S L, Pradhan G K, Narayana C and Ganguli A K 2009 *Solid State Sci.* **11** 562
[30] Wang H H, Wu F and Jiang H 2011 *J. Phys. Chem. C* **115** 16180
[31] Wu X Y, Yin S, Dong Q and Sato T 2013 *Phys. Chem. Chem. Phys.* **15** 20633
[32] Kanhere P, Nisar J, Tang Y X, Pathak B, Ahuja R, Zheng J W and Chen Z 2012 *J. Phys. Chem. C* **116** 22767
[33] Nisar J, Wang B C, Pathak B, Kang T W and Ahuja R 2011 *Appl. Phys. Lett.* **99** 051909
[34] Zhao Y R, Xiang T C and Han P L 2014 *Appl. Mech. Mater.* **457** 202